Robustness vs. Accuracy: Multipath Effects on Land Mobile Satellite Navigation

Alexander Steingass, Bernhard Krach*,Massimo Crisci †

October 10, 2016

Abstract

Knowledge of performance for different signal options in difficult environments is vital for improving modern satellite navigation systems. Currently, the accuracy of the different transmission signals in realistic multipath environments is still not known in current literature. In this study different classical and advanced signals have been simulated using an urban multipath channel model standardized by the International Telecommunication Union (ITU). For the given multipath channel, signal and receiver effects have been investigated.

The performance of GPS C/A and GALILEO open service (OS) signals in this environment has been compared. Additional simulation of wide band navigation signals lead to the uncovering of an important conflict between robustness and accuracy in terms of signal bandwidth. This conflict is signal inherent and not associated to a particular receiver. As a result of this finding an improved satellite signal extension for robust urban navigation has been proposed.

On the receiver side pure line-of-sight conditions have been identified in which a novel particle filter (PF) based receiver shows a comparable performance as a classical delay locked loop (DLL). In a mixture of line-of-sight and shadowing conditions the particle receiver clearly outperformed the classical DLL. For the classical DLL critical scenarios have been identified that are often causing a loss of lock (LOL).

1 Introduction

Multipath propagation and ionosphere influence are two most critical error sources for satellite navigation. Already at the beginning of the development of GALILEO investigations concerning the navigation performance of various signals had been made [1, 2]. Lack of accurate models for signal propagation in urban multipath environments did result in different hypothetical channel models [1]. Their usage in simulations showed an extreme influence of the signal propagation on the navigation accuracy. This exposed the necessity of measurements for the satellite-to-land mobile channel. These measurements have been carried out in [3] and have brought an in-depth understanding of signal propagation in urban, suburban, and rural environments. These measurements have been analyzed [4] and have resulted in a multipath channel model [5] which has been released into the public domain [6]. The International Telecommunication Union (ITU) has standardized this model [7,8].

The development of GALILEO [9] and the modernization of GPS [10] have been accompanied by a long discussion about new wideband signal options. These have resulted into the definition of the GALILEO signal format [11], the invention of GPS M-code for military applications [12], and a second signal L2C on L5 for civil applications [13].

A typical solution for synchronizing a navigation signal would be a conventional delay locked loop (DLL) receiver. These classical DLL receivers [14] have been improved by more multipath selective timing error detectors (TEDs) [15–18]. The development of the multipath estimating DLL (MEDLL) [19] brought about a new class of navigation receivers with a single maximum as a mono-modal estimate. The application of Bayesian estimation receivers [20–22] extended this estimation approach to a multi-modal estimate by using a particle filter (PF). Therefore, we selected the most promising advanced receiver concepts as candidates to be compared with the DLL: The maximum likelihood (ML) receiver and the sequential Bayesian estimation approach implemented by a particle filter (PF). To determine their

*German Aerospace Center - DLR
†European Space Agency - ESA

strengths and weaknesses these receivers have been investigated using new and classical signal formats.

The results of these investigations are summarized in this work. It has been shown that the dynamic fading process of the line of sight (LOS) introduced difficulties to navigate in urban environments. The receivers lost lock, accuracy was extremely degraded, and availability was reduced. Specifically, the wideband signals have shown problems under these conditions. Here, a tradeoff between highly accurate wideband signals and robust narrow band signals has been found. This tradeoff is signal inherent and not dependent on a receiver structure. Critical situations for DLL receivers have been found especially if the receiver is faced with rapid visibility changes.

The work presented in this paper can be used for further improvement of satellite navigation receivers. To further improve both - the accuracy and robustness of the satellite signals, modification of the current satellite signals has been proposed by adding a narrow-band service to the existing wide-band services.

The paper also briefly introduces the channel model [5]. We describe the three used receivers and depict the simulation setup. The results using narrow- and wideband GPS and GALILEO signals will be shown, and conclusions will be given.

2 Multipath channel model

In 2002 we performed extensive multipath channel measurements [3, 4]. From these measurements we have developed a realistic channel model which has been published in [5] and is now standardized by International Telecommunication Union (ITU) recommendation 681-7 [7, 8].

This channel model is based on a randomly generated, artificial scenery and takes into account blockage, reflexions and attenuation introduced by the elements comprised in the scenery.
We generate the artificial scenery where we use house fronts at the road side to model the attenuation (blockage) of the line of sight (LOS). In addition to the house fronts, trees and light poles (also randomly generated) contribute to the LOS attenuation. The used attenuation models are realized deterministically and use the "knife edge" model [23] to calculate the LOS attenuation.
Independently of the attenuating objects, echoes are generated in the artificial scenery. The echo position, location, power and other parameters are generated randomly according to parametrized stochastic processes. These echoes simulate reflexions with a near field deterministic path from the geometry and a randomly varying stochastic part.
In analogy to [24] we defined a typical urban model. Thus we defined a parameter set that defines the artificial scenery like minimum, maximum and average house width and height as well as echo parameters such as location maps for echo probability, power distribution of the echoes to name just a few.
We derived these parameters from the mentioned measurements and we assume that the model represents many big cities worldwide e.g. America, Asia and the Middle East. There are however situations, e.g. Lower Manhattan, where the model fit might be improvable. This can be done by adapting the statistics for the model. In [8] the interface for this extension is standardized.
A detailed description of the model used here we leave outside the scope of this paper. An interested reader is referred to [8] for more details.
To apply the model, a set of parameters needs to be chosen. For best comparability with other publications we kept the parameters from [8] unchanged.
Although selected movement parameters such as speed, acceleration and heading as defined in [8] have to be selected to reflect the simulated application. Again we follow [8] and use the speed profile "ITU P.2145 Car A". This is analyzed and shown in section 4 together with other relevant parameters of the used receivers.

In general, the channel impulse response $h(t, \tau)$ of a multipath channel with a direct path and N echoes can be written as

$$h(t, \tau) = \sum_{i=0}^{N} a_i \cdot \delta(t - \tau_i). \tag{1}$$

Let us denote the transmitted signal $s(t)$ to be the transmitted signal, then the received signal $r(t)$ can be calculated by using equation 1:

$$\begin{aligned} r(t) &= s(t) * h(t, \tau) + n(t) \\ &= \sum_{i=0}^{N} a_i \cdot s(t - \tau_i) + n(t) \ , \end{aligned} \tag{2}$$

where $n(t)$ denotes the zero-mean white Gaussian noise.

3 Receivers

In satellite navigation, precise synchronization at the receiver is crucial for providing accurate time delay estimates and subsequent position determination. In particular the synchronization of the spreading code sequences is important, as they provide unambiguous measures of signal travel time.

The signal processing techniques that are considered for multipath-robust receiver architectures have evolved significantly during the last decades. In general two fundamentally different approaches can be distinguished. The classical methods, which are still employed in most of the satellite navigation receivers today, align the conventional receiver components in a way that mitigates the impact of the multipath reception. In contrast, the advanced receiver concepts rely on estimation techniques, whose principles adhere to optimal methods in statistical signal processing. The estimation methods treat multipath explicitly as something to be estimated from the received signal, such that its effects can be trivially compensated at a later processing stage.

In the following, we introduce the concepts of the simulated receivers.

3.1 Delay locked loop (DLL)

In a conventional navigation receiver a combination of a DLL and a frequency/phase locked loop (FLL/PLL) is used to aid the estimation of the signal travel times [14]. The DLL is designed to keep track of the timing of the received signal by solving the following optimization problem

$$\hat{\tau}_0^{\mathrm{DLL}}(t) = \arg\min_{\tau_0} \int_t^{t+T} |r(t) - a_0 s(t-\tau_0)|^2 \, \mathrm{d}t \ . \quad (3)$$

The FLL/PLL is used to compensate frequency and phase variations of the signal. The synchronization is continuously refined by the estimate of the actual timing mismatch, which is obtained from the timing error detector (TED) of the DLL. The slope of the TED is designed to be an approximation to the derivative of the cross-correlation function between the received signal and a local replica. This is achieved by means of the differential quotient, for example by employing two local replica $s(t-\tau_0+\Delta\tau)$ and $s(t-\tau_0-\Delta\tau)$, that is one in advance (early) and one in delayed (late) stage by $\Delta\tau$, in order to sample the cross-correlation function at the respective values. Figure 1 illustrates the DLL concept. An inphase/prompt correlation is commonly used to feed the frequency/phase estimation of the FLL/PLL.

Most of the conventional multipath mitigation techniques align the TED of the DLL to the signal received in the multipath environment in some way. Examples are the narrow correlator [15], the strobe correlator [16], the gated correlator [17], or the pulse aperture correlator [18], to name a few.

However, in any case multipath reception with delays much smaller than the chip duration of the spreading code leads to a distortion of the TED, which introduces a bias in the time delay estimate of the DLL. Though being susceptible to multipath errors, the DLL-based receiver concept has been proven to be efficient and reliable whilst being of little complexity [14]. Hence, its use is widespread and it can be regarded as the standard for today's satellite navigation receivers.

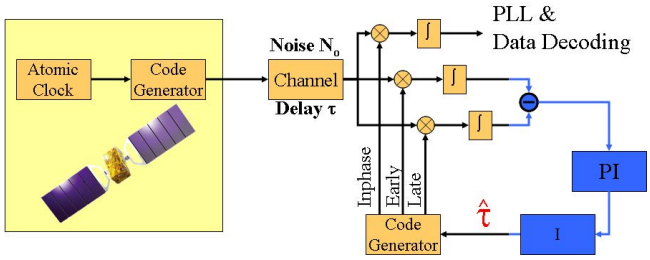

Figure 1: Signal generation, signal propagation through the channel, and signal reception with a DLL receiver..

3.2 Maximum Likelihood Estimation

The concept of maximum likelihood (ML) multipath estimation is an extension of the above DLL concept. It has drawn substantial research interest since the first approach was proposed in [25]. Despite varying details the objective is the same for all ML approaches, namely to find the parameters that maximize probability of the given observation $\mathbf{r}_k$ conditioned on state of the channel $\mathbf{x}_k$:

$$\hat{\mathbf{x}}_k^{\mathrm{ML}} = \arg\max_{\mathbf{x}_k} \{p(\mathbf{r}_k|\mathbf{x}_k)\} \ , \quad (4)$$

where $\mathbf{r}_k$ is a sampled sequence of the received signal $r(t)$ in an interval of duration T according to (2) and k denotes the discrete time index of the interval.

The signal parameters that characterize the channel at this time, that is, specifically the delays τ_i, and the coefficients a_i are thereby assumed as being constant throughout the observation period, such that

$$\mathbf{x}_k \widehat{=} \{\tau_i, a_i, i = 0, \ldots, N\} \ . \tag{5}$$

To solve (4) different optimization strategies exist, which basically characterize the different approaches. Most of these maximization algorithms are based on iterative techniques such as the space alternating generalized expectation maximization algorithm (SAGE) [26] and the Newton type methods. The multipath estimating DLL (MEDLL) [25] uses an iterative maximization method similar to the SAGE algorithm. Newton-type methods with efficient analytical expressions for the gradient and Hessian terms have been considered in [27] and have been chosen for the assessment that is performed within this paper. Further, ML algorithms have been reported in [28, 29].

For the ML approach the likelihood function is according to (2) the complex-normal distribution

$$p(\mathbf{r}_k|\mathbf{x}_k) = \mathcal{N}\left(\sum_{i=0}^{N} a_i \cdot \mathbf{s}(\tau_i); \sigma^2\right) \ , \tag{6}$$

with $\mathbf{s}(\tau_i)$ being a discrete-time representation of $s(t - \tau_i)$ in an interval of duration T and σ^2 being the variance of the sampled noise.

As derived in [27] the Newton-type method starts at an initial sample point on the so-called likelihood cost-function, which in our case is given by $\mathbf{L}(\mathbf{x}_k) = -\log\left(p(\mathbf{r}_k|\mathbf{x}_k)\right)$. Hence, a maximization of (6) is equivalent to the minimization of $\mathbf{L}(\mathbf{x}_k)$. By eliminating the dependences with respect to the complex amplitudes a_i in an analytical fashion according to [27] the optimization with respect to the delays τ_i descends iteratively toward a point of convergence. At each iteration n the estimate $\hat{\mathbf{x}}_k^n$ is refined using

$$\hat{\mathbf{x}}_k^{(n+1)} = \hat{\mathbf{x}}_k^{(n)} - \nu \left(\mathbf{H}(\hat{\mathbf{x}}_k^{(n)})\right)^{-1} \nabla\mathbf{L}(\hat{\mathbf{x}}_k^{(n)}) \ , \tag{7}$$

with the gradient $\nabla\mathbf{L}(\mathbf{x}_k)$, the Hessian $\mathbf{H}(\mathbf{x}_k)$, and the step-size parameter $\nu > 0$. Finally the estimate attains the point of convergence and the iteration is stopped according to specific criteria, for example, as soon as the refinement is below a defined threshold. This procedure is carried out at each time instant k independently, such that at each interval an estimate of $\mathbf{x}_k$ is obtained, which relies only on the recent observation $\mathbf{r}_k$ and thus does not take into account any prior information from previous intervals.

To determine the (unknown) number of impinging echoes the estimate $\hat{\mathbf{x}}_k^{\mathrm{ML}}$ is computed for various hypotheses N and the best matching solution is chosen by a likelihood ratio test [30].

In our implementation of the ML method we apply complexity reduction methods according to [31], which allow for operating the algorithm on a compressed variant of the received signal. To obtain the compressed signal, the original received signal is fed to a bank of signal matched correlators, where each of them represents a local replica of the received signal, and that are spaced equally with respect to signal delay across the chip duration of the navigation signal. The estimation is then performed based on the output of the bank of correlators.

3.3 Sequential Bayesian Estimation

The sequential estimation approach is motivated by the fact that though the channel is time-variant, its evolution and thus its state are not independent from one observation period to another. Hence, these temporal dependences may be exploited to refine the estimation. The key idea is to combine information derived from the current observation in terms of the likelihood function $p(\mathbf{r}_k|\mathbf{x}_k)$ with some apriori information $p(\mathbf{x}_k)$ according to the fundamental theorem of Bayes [32], which has been widely used in modern detection and estimation applications [33] in order to determine the aposteriori probability density function (PDF)

$$p(\mathbf{x}_k|\mathbf{r}_k) = \frac{p(\mathbf{r}_k|\mathbf{x}_k)p(\mathbf{x}_k)}{p(\mathbf{r}_k)} \ . \tag{8}$$

In case $p(\mathbf{x}_k)$ is derived from the entire history of channel observations $\mathbf{R}_k \widehat{=} \{\mathbf{r}_{k'}, k' = 1, \ldots, k\}$, the framework of sequential Bayesian estimation is a suitable choice to achieve this goal and it has been proposed by [20,21] for tracking parameters of navigation signals in multipath environments.

The sequential Bayesian approach determines $p(\mathbf{x}_k|\mathbf{R}_k)$, that is, the aposteriori PDF of the channel parameters $\mathbf{x}_k$ conditioned on the entire sequence of past channel observations $\mathbf{R}_k$, in a recursive fashion. The characterization of the channel, which accounts for the constraints and dependencies during its temporal evolution, enters the algorithm in terms of the statistical channel model $p(\mathbf{x}_k|\mathbf{x}_{k-1})$ [22]. Due to the probabilistic approach all potential channel configurations are considered simultaneously by the PDF representation and hence past channel information

is preserved over time. In particular this approach allows for keeping track of ambiguous situations by means of a multi-modal PDF, which is in contrast to the DLL and the ML receiver that are only able to provide point estimates.

Using the aposteriori PDF from the last time instant $p(\mathbf{x}_{k-1}|\mathbf{R}_{k-1})$ and the channel model the a-priori PDF of the channel parameters is computed during the prediction-step of the algorithm:

$$p(\mathbf{x}_k|\mathbf{R}_{k-1}) = \int p(\mathbf{x}_k|\mathbf{x}_{k-1})p(\mathbf{x}_{k-1}|\mathbf{R}_{k-1})\mathrm{d}\mathbf{x}_{k-1}. \quad (9)$$

The update-step of the algorithm joins the apriori PDF with the likelihood function $p(\mathbf{r}_k|\mathbf{x}_k)$, which represents the current observations according to (6). The Bayes theorem (8) is used to obtain the current aposteriori PDF of the channel parameters which gives

$$p(\mathbf{x}_k|\mathbf{R}_k) = \frac{p(\mathbf{r}_k|\mathbf{x}_k)p(\mathbf{x}_k|\mathbf{R}_{k-1})}{p(\mathbf{r}_k|\mathbf{R}_{k-1})} \ . \quad (10)$$

Once the a-posteriori PDF is evaluated, either the channel configuration that maximizes it can be determined which is the so-called maximum a-posteriori (MAP) estimate or the minimum mean square error (MMSE) estimate can be chosen:

$$\hat{\mathbf{x}}_k^{\mathrm{MMSE}} = \int \mathbf{x}_k p(\mathbf{x}_k|\mathbf{R}_k)\mathrm{d}\mathbf{x}_k \ . \quad (11)$$

The MMSE estimate has been chosen for this paper, as in our simulations MMSE was more robust than the MAP estimate. To implement the sequential Bayesian approach we have employed a particle filter (PF) according to [34] and the corresponding receiver type will be referred to as PF receiver in the sequel of the paper. An alternative PF implementation for static channel scenarios can be found in [35].

A PF solves the Bayesian filtering equations based on the principle of importance sampling [36] and thus inherently implements only a suboptimal approximation of the optimal Bayesian solution [37]. In a PF the a-posteriori PDF at step k is represented as a sum, and is specified by a set of N_p particles:

$$p(\mathbf{x}_k|\mathbf{R}_k) \approx \sum_{\mu=1}^{N_p} w_k^\mu \delta(\mathbf{x}_k - \mathbf{x}_k^\mu) \ , \quad (12)$$

where each particle with index μ has a state $\mathbf{x}_k^\mu$ and has a weight w_k^μ. For $N_p \to \infty$ the approximate a-posteriori PDF approaches the true a-posteriori PDF, hence the number of particles N_p has to be chosen in a trade-off between performance and complexity.

Following [37] the particles are generated randomly from the so-called proposal density $q(\mathbf{x}_k|\mathbf{x}_{k-1}^\mu, \mathbf{r}_k)$, such that their respective weights are calculated via

$$w_k^\mu \propto w_{k-1}^\mu \frac{p(\mathbf{r}_k|\mathbf{x}_k^\mu)p(\mathbf{x}_k^\mu|\mathbf{x}_{k-1}^\mu)}{q(\mathbf{x}_k^\mu|\mathbf{x}_{k-1}^\mu, \mathbf{r}_k)} \ . \quad (13)$$

The choice of the proposal density is crucial for the performance of the PF and is, thus, characteristic for the specific realization of the filtering algorithm. A common choice is the so-called sequential importance re-sampling particle filter (SIR-PF) [37] that we have followed in our implementation. In the SIR-PF the proposal density is chosen to be $p(\mathbf{x}_k|\mathbf{x}_{k-1} = \mathbf{x}_{k-1}^\mu)$, which follows directly from the channel process characteristics. At each instance k the SIR-PF incorporates the recent observation in terms of the received signal $\mathbf{r}_k$ in the calculation of the weight w_k^μ, which can be shown to be the likelihood function $p(\mathbf{r}_k|\mathbf{x}_k^\mu)$ (6).

The nominal performance of PF methods in this context has been studied in detail by a couple of papers before. In [38] the statistical multipath error envelope has been assessed and compared against a DLL using a Narrow and a Strobe correlator. As the results of a similar assessment [20] shows that the PF approaches the Cramer-Rao lower bound (CRLB) for an increasing number of employed particles. In addition [35] derives the computation of the applicable Posterior CRLB and studies the amount of particles needed to converge.

The PF estimates the delays τ_i of the impinging path and considers the earliest estimate as the LOS delay τ_0. The later estimates are treated as the delays of the echo paths. As the characteristic for the land mobile scenario, all echoes are assumed to experience a typical life cycle [3], that is, echoes are created and erased dynamically according to probabilistic models. In the PF according to [34], an echo detection is included implicitly, thus an explicit estimation of the number of impinging echoes is not required here. This is in contrast to [35], where the number of echoes is assumed to be known perfectly. However, the number of maximum detectable echoes N_m is limited due to complexity constraints and it has been shown in [34] that the PF receiver performance tends to saturate rapidly, if more than one simultaneous echo is detectable by the receiver.

In our implementation of the PF we take advantage of the same complexity reduction methods that

have been employed for the ML receiver [31], that is, specifically the likelihood function is computed from the output of a correlator bank, which reduces the effort for the PF computations significantly [38].

4 Simulation setup

We simulated a car drive in an urban environment. For this purpose we divided the route into 10 segments, each lasting for 180 seconds. The total simulation time of 30 minutes has been considered as long enough for sufficient statistics. Every segment was begun with a perfect synchronized receiver. This segment was used for the error statistics as long as the receiver was tracking the signal. This detection was done manually after simulation.

The PF receiver was using 25 correlators set to a coherent integration time of 10 ms to follow dynamic channel changes. The PF receiver considered $[0, 1, 2, 3]$ reflections as hypothesis it was using 1000 particles. The DLL was set to a filter bandwidth of 1 Hz and a correlator spacing of 0.15 chips.

To realize a critical multipath and shadowing situation we simulated a satellite at an elevation of 10°. To remove the influence of a specific azimuth we simulated a circular route which covered every azimuth equally. To realize a typical stop and go situation in a city a speed profile with high, medium, and slow speed periods as well as stop periods was defined (see figure 2). All other parameters of the multipath channel had been set as recommended in the standard [8]. The nominal C/N_0 is representing the un-shadowed reception; it was set to 45 dBHz. Further attenuation or blocking of the LOS signal are automatically calculated by the channel model itself depending on the actual reception situation. Thus the LOS power level is changing over time.

Four different global navigation satellite system (GNSS) signal types were simulated: Two of them were in the L1 frequency band and two of them in Galileo's E5 band [11]. Specifically, the simulations were run with the GPS C/A code signal (BPSK(1)), the Galileo BOC(1,1) signal, the AltBOC(10,10) signal using its full bandwidth, and a BPSK(10) signal which uses the E5b frequency band [11].

5 Results

In this section we will present the results of our simulations.

5.1 Shadowed signal reception

A very difficult situation for GNSS receivers occurs when the LOS signal is shadowed and the reflections become stronger than the LOS. Figure 3 shows such a situation: The LOS is shadowed by house fronts and the received signal contains components from the LOS as well as from reflections. A standard DLL receiver in this situation is misled by the reflection and shows severe errors while a PF receiver successfully estimates the reflection. Hence some of the particles contain an estimate for the weak LOS. This receiver can correct the effect caused by the reflections. Moreover, the strong reflection leads to particles with a high likelihood although the LOS is weak. Therefore, the PF receiver is clearly outperforming the DLL in these situations.

5.2 Accuracy versus robustness

Newly designed signals for satellite navigation are designed for high-accuracy navigation. This goal is usually reached by an increase of the signal bandwidth [11, 12]. This leads to two important consequences: Due to the higher bandwidth the chip length will be shorter which results (with the same given C/N_0) in a higher detector gain [14] that reduces the variance of the navigation error. Further, the sensitivity to multipath is reduced indeed: Let $s(t)$ be the transmitted satellite signal and $h(t, \tau)$ be the channel impulse response. Then the received signal $r(t)$ is

$$r(t) = s(t) * h(t, \tau) + n(t). \tag{14}$$

The correlator output $c(t, \tau)$ of the receiver is [14]:

$$\begin{aligned} & c(t, \tau) \\ = \; & (s(t) * h(t) + n(t)) * s^*(-t - \tau) \\ = \; & s(t) * s^*(-t - \tau) * h(t) + \\ & n(t) * s^*(-t - \tau) \\ = \; & \underbrace{\varphi_{ss}(t - \tau) * h(t)}_{\text{filtered channel}} + \\ & \underbrace{n(t) * s^*(-t - \tau)}_{\text{col. noise term}} \end{aligned} \tag{15}$$

where $\varphi_{sg}(\tau) = \int_{-T}^{T} s(t) \cdot g^*(t + \tau) dt$ is the cross-correlation function (CCF) between $s(t)$ and $g(t)$ and φ_{ss} is the auto correlation function (ACF) of $s(t)$.

The interpretation of equation 15 is that the correlator output is the channel impulse response filtered

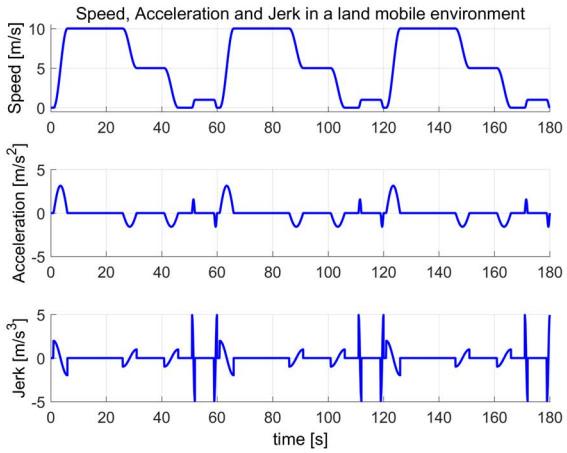

Figure 2: Speed profile used periodically for the simulations.

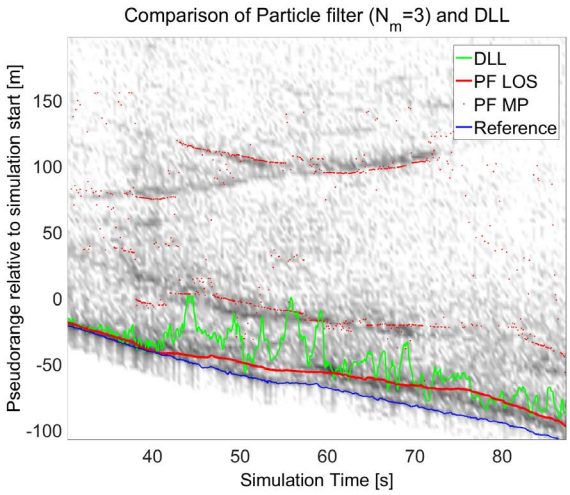

Figure 3: Reception of the shadowed signal in the presence of strong reflections: The DLL estimate is represented by (green), the PF LOS estimate (red), and the multipath estimates of the PF (red dots). Also shown is the reference (blue) being the true pseudorange. In the background the measured channel impulse response (100 MHz bandwidth) is shown.

by the autocorrelation function of the signal observed in the presence of colored noise. When the signal bandwidth is increased the autocorrelation function is shortened which leads to a higher suppression of multipath components. This property can be seen in figure 4. In this figure the autocorrelation function of GPS C/A, Galileo E5 (full band), and GPS L5 which equals GALILEO E5b is displayed together with the channel impulse response of the multipath channel. This will increase the navigation accuracy **as long as** the LOS is present, because reflections that reach the receiver antenna longer delayed are suppressed while the LOS is unaffected.

In the case of shadowing we observe the opposite situation: An echo that has a longer delay than the ACF will be detected by the receiver independent of the LOS. Therefore, the short ACF suppresses[1] these reflections but the LOS is missing or at least attenuated. This results in a lack of useful energy at the correlator output and the DLL is losing lock quickly. Figure 5 shows an example of such a situation: The user is losing the LOS by shadowing and the receivers relying on wideband signals are losing lock. The receiver synchronizing a narrow band signal (GPS C/A) is building up a larger error but stays within the hold range of the DLL. When the LOS comes back after a short period it resynchronizes the signal if the LOS stays long enough.

We have repeated this simulation for different azimuths and the loss of lock for the high bandwidth signals occurred always when the LOS was blocked. Therefore we conclude that it is impossible to synchronize these signals in a blockage situation. From a user point of view this results in a trade off between higher accuracy in LOS situations by using high signal bandwidths (e.g. 80 MHz-GALILEO E5) and robust navigation in shadowing situations by narrow bandwidths (e.g. 1 MHz - GPS C/A or 2 MHz GALILEO BOC (1,1)). In the L1 band the user can select the signal to be used but unfortunately in the E5, L5 bands only a wide band service is implemented at the moment. Thus, from a user point of view an additional narrow band service on E5 or L5 might be useful.

[1] This suppression capability was intended when designing the wideband signals.

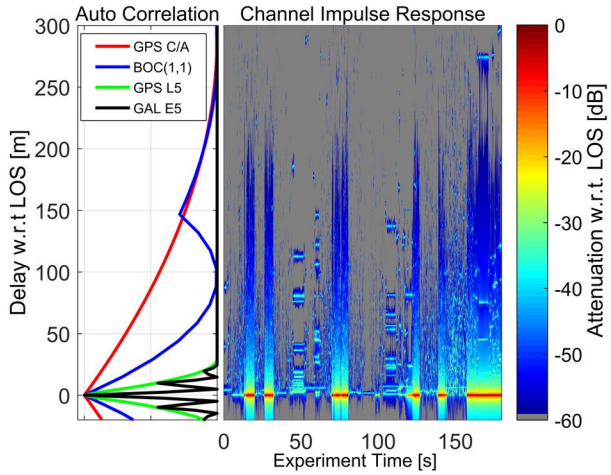

Figure 4: Channel impulse response (right) plotted in the same delay scale as the signal $|\mathrm{ACF}|^2$ (left). The signal power is normalized and since the baseband ACF of GPS P-code (L1,L2), GPS L5 (L2C) and GAlILEO E5b is identical. This common ACF is named "GPS L5" (green). The GALILEO OS on L1 is realized by a BOC(1,1) signal (blue).

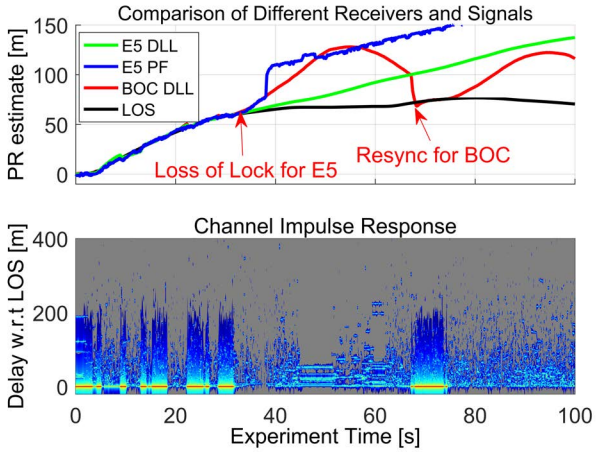

Figure 5: Receivers that use the wide band signal E5 are losing lock caused by the loss of the LOS. The DLL that uses the GALILEO BOC(1,1) signal can resynchronize after the LOL.

5.3 Comparison BOC(1,1) versus BPSK(1)

As shown in the previous section the increase of signal bandwidth can have enormous impact on the robust reception of the satellite signal. This brought another improvement of modern satellite navigation to the focus of our interest: The change from BPSK (1) signals (used in GPS) to BOC signals, namely from GPS C/A to GALILEO BOC (1,1).

We simulated both signal options using the identical channel described in section 4. Figure 6 shows the result of these simulations: It can be seen that for all

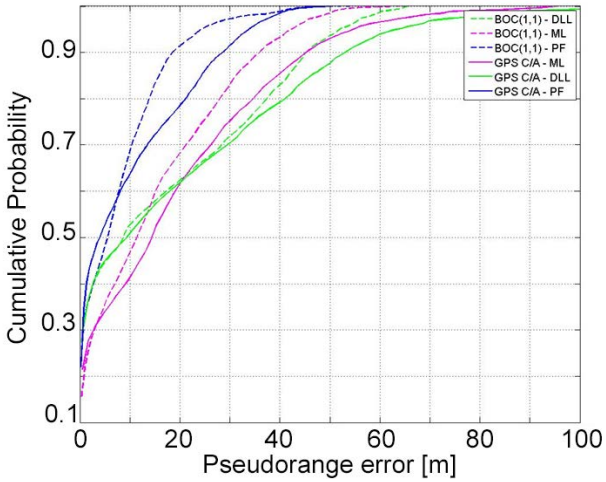

Figure 6: Comparison between GPS C/A code and GALILEO BOC(1,1).

three receivers the BOC(1,1) signal outperforms the C/A code signal in terms of accuracy. In terms of robustness the increase of the bandwidth from 1 MHz to 2 MHz had a negligible effect on the availability of the navigation service. Revisiting figure 4 confirms this result: The ACF of the BOC (1,1) signal is wide enough to collect most of the channels energy for robust navigation and is narrow enough to allow a good navigation performance.

5.4 Improvements on the satellite signal

In the previous section we discovered a principle tradeoff between robust narrow band and accurate wideband signals. Because this problem is signal inherent and not system specific it affects both GPS

and GALILEO. Hence, it is obvious that a potential modification on the satellite signal might solve this tradeoff. It would go beyond this paper to propose a ready to use solution for this problem, which would need extensive research and field trials. However, we want to contribute to an upcoming discussion with signal extensions.

Our assumption is that an ionospheric correction is beneficial even for mass market receivers in difficult reception environments. Thus we propose to improve a robust dual frequency reception: We figured out, that the invention of the BOC (1,1), signal to satellite navigation improved its accuracy in the multipath channel while keeping a reasonable robustness. Therefore, and for best compatibility, a possible solution is to insert a narrow band BOC (1,1) service overlaying the wideband services of E5-band signals of GALILEO. For GPS L5 a close solution would certainly be a C/A signal overlaid at the center frequency of L5. Figure 7 shows two possible

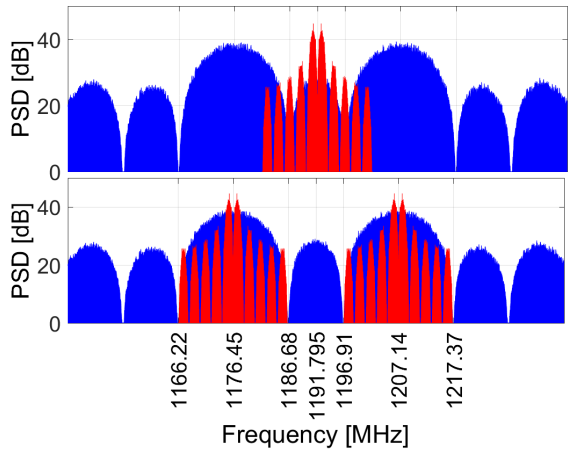

Figure 7: Possible signal extensions in the GALILEO E5 band.

extensions of the GALILEO E5 signal:

- Possibility 1 uses a center frequency of 1191.795 MHz to transmit an additional BOC (1,1) signal. The advantage of this option is a low spectral interference to the existing E5 services. The disadvantage is that a receiver that uses one side band only (e.g. E5b for the safety of life (SOL) service) would need a wider input bandwidth and would access an unprotected band for the narrow band signal.
- Possibility 2 uses center frequencies of 1176.45 MHz and 1207.14 MHz to insert two BOC(1,1) signals into the E5 band. The advantage of this approach is that no modification of the radio frequency (RF) receiver front-end would be necessary. The disadvantage is of course the doubled necessary signal power.

5.5 Receiver performance

In this section we investigate the performance of the different receivers used on the same channel. As a measure we use the root mean squared error ψ which is derived from N samples of the estimated pseudorange $\hat{\tau}(k)$ and the real pseudorange $\tau(k)$ at every time instance k:

$$\psi = \frac{1}{N}\sqrt{\sum_{k=1}^{N}\left(|\hat{\tau}(k) - \tau(k)|\right)^2} \tag{16}$$

Figure 8 shows the simulation performance for a

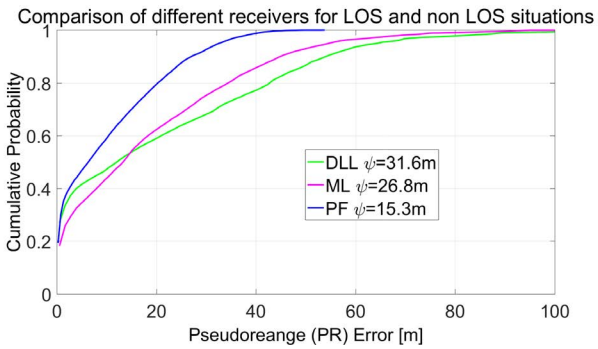

Figure 8: Comparison of the receiver performance for GALILEO BOC(1,1) over the complete channel covering LOS and shadowed situations.

mixture of LOS and shadowed situations. For the whole channel the PF clearly outperforms the DLL and the ML. For every estimation period the ML receiver uses independent measurements without history. Therefore it cannot benefit from the previous estimates like the PF receiver, in particular with respect to the presence of multipath. As the coherent observation intervals for the ML and PF receiver are the same, the ML receiver is more susceptible to noise than DLL and PF. The comparison between DLL and ML receiver brings a more differentiated result: If the channel shows only small echo delays

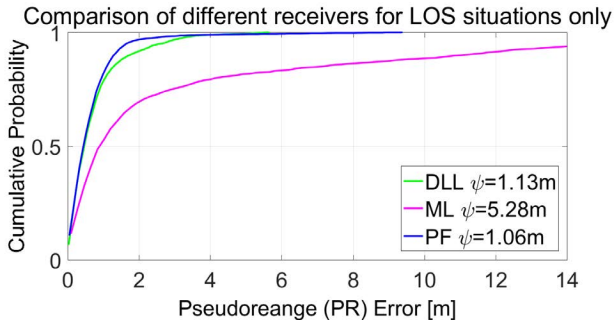

Figure 9: Comparison of the receiver performance for GALILEO BOC(1,1), LOS situations only.

the ML receiver can hardly estimate them properly, as the overall error is more dominated by noise than by multipath bias. Therefore the DLL is in advantage here and shows small errors. Increasing echo delays result in higher errors dominated by multipath bias for the DLL, whereas the ML receiver can estimate them better, so in a comparison the break even is reached for about 15 m error.
In contrast to the mixed propagation situation a different result can be seen when the same simulations are evaluated for LOS situations only (figure 9). Here the PF and the DLL receivers show a comparable performance whereas the ML receiver still shows erroneous estimates.
As discussed in [19, 38] in practice the performance of the ML receiver may be improved by extending its equivalent observation interval beyond the actual coherence time of the channel, in order to reduce its susceptibility to noise.

From this we can conclude that in LOS situations it is unlikely to receive a strong echo in the order of the LOS and the DLL receiver is sufficient to synchronize the signal. In shadowing situations the PF receiver is able to estimate the channel properly and thus can suppress multipath effects. This knowledge can be used in a receiver to adopt the receiver complexity to the channel condition: In a shadowing situation a PF receiver should be used whereas in a LOS situation a DLL receiver is sufficient. This selective usage of the different receiver concepts would improve battery lifetime. Further, one can combine PF and DLL in the same chip by flexible use of correlators. This would allow a receiver layout that can receive n_s shadowed satellites by using a PF and n_v visible satellites by using a DLL. Because it is unlikely that all satellites are shadowed this concept can optimize the complexity. It would reduce chip size of the receiver by approximately $1 - \frac{n_s}{n_s+n_v}$ assuming that the complexity of a PF is high compared to a DLL.

5.6 Critical situations for DLLs

During the simulations we have identified a critical situation for a DLL based receiver: When the received signal is weak the navigation accuracy is decreased. In this state the receiver can show a significant error. If the LOS comes back the detector of the DLL will generate a big correction signal to bring the DLL back to the right pseudorange. If this LOS period is longer than its settling time it will synchronize correctly. If the LOS period is shorter than the settling time the big correction signal during the LOS period is loaded into the integrator of the DLL; when exiting this short LOS period the detector signal becomes weak again and the loop behavior is then dominated by the previous correction signal stored in the integrator. In this moment the DLL will execute this "last command" and will lose the lock. We call this short line of sight hit (SLOSH).

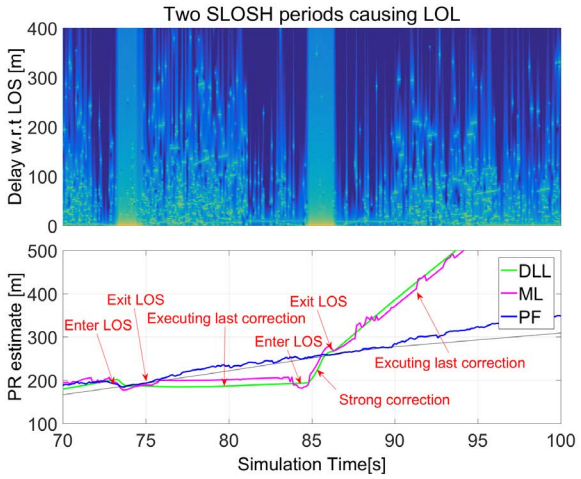

Figure 10: short line of sight hit – GALILEO BOC(1,1).

Figure 10 shows a DLL and a PF receiver in a double SLOSH situation. The first SLOSH loads a medium correction signal into the integrator which cannot settle during the SLOSH. It executes the last correction command and builds up an increasing error in the following non-LOS period. When the second SLOSH occurs the correction command of the detector is big and the DLL tries to settle. Again the

SLOSH is too short for settling and the receiver is losing the lock. The PF receiver is unaffected by the SLOSH. In contrast to a DLL it does not use a "flywheel effect" but a Bayesian filter, which combines correctly the apriori and the aposteriori likelihoods. The only observable effect is a widening of the distribution function and a higher noise during the non LOS period.

6 Conclusion

We have introduced a new particle- based receiver concept and tested this new receiver together with a classical delay locked loop (DLL) and a maximum likelihood multipath estimation DLL in a multipath environment. We have shown that the particle receiver is clearly outperforming the DLL and the maximum likelihood (ML) receiver in shadowed situations. In a line of sight situation a DLL and a particle receiver are showing a comparable performance. We found a tradeoff between accurate and robust navigations signals: Wideband signals show higher accuracies if the line of sight (LOS) is present, narrow band signals show a higher robustness if the LOS is shadowed. As a result of this finding a potentially improved satellite signal extension for robust urban navigation has been suggested to allow both: Robust navigation using an additional narrow band signal and accurate navigation using the existing wideband signal. This may serve as robust and accurate means of navigation in a stand alone configuration or contribute as component to multi-sensor navigation systems, which will push the overall performance in land mobile navigation even further.
Further, we compared the GPS C/A service with a GALILEO binary offset coding (BOC) (1,1) signal. While being robust enough the BOC (1,1) showed a better performance in the multipath environment by means of simulation. In a last step we have identified a critical situation for a DLL: The short line of sight hit (SLOSH). This happens when a DLL envisages for a period smaller than the settling time of the DLL a LOS situation occurs. After this event a loss of lock (LOL) is very likely.

Acknowledgments

The work reported in this paper has been supported under a contract of the European Space Agency in the frame of the European global navigation satellite system (GNSS) Evolutions Programme. We want to thank all people involved, especially Francesca Zanier (ESA) for fruitful and valuable input to this project. The views presented in the paper represent solely the opinion of the authors and should be considered as R&D results not necessarily impacting the present EGNOS and Galileo system design.

References

[1] R. Schweikert and T. Woerz, "Signal design and transmission performance study for GNSS–2 on digital channel model for data transmission," European Space Agency ESA, Tech. Rep., 1998.

[2] R. Schweikert, T. Wörz, R. De Gaudenzi, A. Steingass, and A. Dammann, "On signal structures for gnss-2," International Journal of Satellite Communications IJSC, vol. 18, no. 4-5, pp. 271–291, 2000. [Online]. Available: http://dx.doi.org/10.1002/1099-1247(200007/10)18:4/5⟨271::AID-SAT658⟩3.0.CO;2-Y

[3] A. Steingass and A. Lehner, "Measuring Galileo's multipath channel," in Proceedings of the the European Navigation Conference, Graz, Austria, Apr. 2003.

[4] ——, "Measuring the navigation multipath channel - a statistical analysis," in Proceedings of the ION GPS/GNSS conference. Long Beach, California, USA: Institute of Navigation, Sep. 2004.

[5] ——, "A channel model for land mobile satellite navigation," in Proceedings of the the European Navigation Conference. Munich, Germany: German Institute of Navigation (DGON), Jul. 2005.

[6] Alexander Steingass and Andreas Lehner. (2012, Apr.) Satellite navigation multipath channel models. [Online]. Available: http://www.kn-s.dlr.de/satnav/

[7] ITU-R, "Propagation data required for the design of earth-space land mobile telecommunication systems," International Telecommunication Union ITU, Geneva, Switzerland, Recommendation 681-7, Oct. 2009.

[8] ——, "Model parameters for an urban environment for the physical-statistical wideband LMSS

model in recommendation ITU-R P.681-7," International Telecommunication Union ITU, Geneva, Switzerland, Report P.2145, Oct. 2009.

[9] E. Commission, "Towards a trans-european positioning and navigation network: a european strategy for global navigation satellite systems (GNSS)." Communication from the Commission to the Council and the European Parliament, Jan. 1998, COM (98) 29 final. [Online]. Available: http://aei.pitt.edu/6801/

[10] Office of Space Commercialization. (2011, Jan.) GPS Modernization. [Online]. Available: http://www.space.commerce.gov/gps/modernization.shtml

[11] GSA, "Signal in space interface control document," European Commission, Tech. Rep., 2010. [Online]. Available: http://ec.europa.eu/enterprise/policies/satnav/galileo/open-service/index_en.htm

[12] J. Betz, "Design and performance of code tracking for the GPS M code signal," MITRE, Tech. Rep., Sep. 2000. [Online]. Available: http://www.mitre.org/work/tech_papers/tech_papers_00/betz_codetracking/

[13] Global Positioning System Wing (GPSW) Systems Engineering & Integration. (2010, Jun.) Interface specification IS-GPS-200 – Revision E. [Online]. Available: www.gps.gov/technical/icwg/IS-GPS-200E.pdf

[14] B. W. Parkinson and J. J. Spilker, Global Positioning System: Theory and Applications I and II, ser. Progress in Astronautics and Aeronautics. Washington DC, USA: American Institute of Aeronautics and Astronautics Inc., 1996, vol. 163.

[15] A. van Dierendonck, P. Fenton, and T. Ford, "Theory and performance of narrow correlator spacing in a GPS receiver," in Proceedings of the ION national technical meeting NTM, San Diego, California, USA, 1992.

[16] L. Garin, F. van Diggelen, and J. Rousseau, "Strobe and Edge correlator multipath mitigation for code," in Proceedings of the ION GPS/GNSS conference, Kansas City, Missouri, USA, 1996, pp. 657–664.

[17] G. MacGraw and M. Brasch, "GNSS multipath mitigation using gated and high resolution correlator concepts," in Proceedings of the ION national technical meeting NTM, San Diego, California, USA, 1999.

[18] J. Jones, P. Fenton, and B. Smith, "Theory and performance of the Pulse Aperture Correlator," in NovAtel Technical Report, NovAtel Inc., Calgary, Alberta, Canada, 2004.

[19] R. van Nee, "The multipath estimating delay lock loop," in Proceedings of the IEEE Second International Symposium on Spread Spectrum Techniques and Applications ISSTA, Dec. 1992, pp. 39–42.

[20] P. Closas, C. Fernandez-Prades, and J. Fernandez-Rubio, "Bayesian DLL for multipath mitigation in navigation systems using particle filters," in Proceedings of the IEEE International Conference on Acoustics, Speech and Signal Processing ICASSP, Toulouse, France, May 2006.

[21] M. Lentmaier, B. Krach, P. Robertson, and T. Thiasiriphet, "Dynamic multipath estimation by sequential monte carlo methods," in Proceedings of the ION GPS/GNSS conference, Fort Worth TX, USA, Sep. 2007.

[22] B. Krach and R. Weigel, "Markovian channel modeling for multipath mitigation in navigation receivers," in Proceedings of the 3rd European Conference on Antennas and Propagation (EUCAP 2009). Berlin, Germany: VDE Verlag, Mar. 2009.

[23] D. M. Pozar, Microwave Engineering. New York, USA: John Wiley & Sons, Inc., 2004.

[24] COST 207, WG1, "Proposal on channel transfer functions to be used in GSM tests," CEPT Paris, Tech. Rep., 1986.

[25] D. van Nee, J. Siereveld, P. Fenton, and B. Townsend, "The multipath estimating delay lock loop: Approaching theoretical accuracy limits," in Proceedings of the IEEE Positioning and Location Symposium PLANS, Las Vegas NV, USA, 1994, pp. 246–251.

[26] J. Fessler and A. Hero, "Space-alternating generalized expectation-maximization algorithm," IEEE Transactions on Signal Processing, vol. 42, no. 10, pp. 2664–2677, Oct. 1994.

[27] J. Selva, "An efficient Newton-type method for the computation of ML estimators in a uniform linear array," IEEE Transactions on Signal Processing, vol. 53, no. 6, pp. 2036–2045, Jun. 2005.

[28] P. Fenton and J. Jones, "The theory and performance of NovAtels Vision Correlator," in Proceedings of the ION GPS/GNSS conference, Long Beach CA, USA, Sep. 2005, pp. 2178–2186.

[29] L. Weill, "Achieving theoretical bounds for receiver-based multipath mitigation using Galileo OS signals," in Proceedings of the ION GPS/GNSS conference, Fort Worth Tx, USA, Sep. 2006, pp. 1035–1047.

[30] P. Stoica, Y. Selen, and J. Li, "On information criteria and the generalized likelihood ratio test of model order selection," IEEE Signal Processing Letters, vol. 11, no. 10, pp. 794–797, 2004.

[31] J. Selva, "Complexity reduction in the parametric estimation of superimposed signal replicas," Elsevier Science: Signal Processing, vol. 84, no. 12, pp. 2325–2343, 2004.

[32] M. Bayes and M. Price, "An essay towards solving a problem in the doctrine of chances. By the late Rev. Mr. Bayes, F.R.S. communicated by Mr. Price, in a letter to John Canton, A.M.F.R.S." Philosophical Transactions, vol. 53, pp. 370–418, 1763. [Online]. Available: www.stat.ucla.edu/history/essay.pdf

[33] H. L. van Trees, Detection, Estimation, and Modulation Theory. New York USA, London UK, Sydney AU: John Wiley & Sons, Inc., 1968.

[34] B. Krach, P. Robertson, and R. Weigel, "An efficient two-fold marginalized bayesian filter for multipath estimation in satellite navigation receivers," EURASIP Journal on Advances in Signal Processing, vol. 2010, no. 1, p. 287215, 2010. [Online]. Available: http://asp.eurasipjournals.com/content/2010/1/287215

[35] P. Closas, C. Fernandez-Prades, and J. Fernandez-Rubio, "A Bayesian approach to multipath mitigation in GNSS receivers," IEEE Journal of Selected Topics in Signal Processing, vol. 3, no. 4, pp. 695–706, Aug. 2009.

[36] A. Doucet, N. de Freitas, and N. Gordon, Eds., Sequential Monte Carlo Methods in Practice. New York, USA: Springer, 2001.

[37] S. Arulampalam, S. Maskell, N. Gordon, and T. Clapp, "A tutorial on particle filters for online nonlinear/non-Gaussian Bayesian tracking," IEEE Transactions on Signal Processing, vol. 50, no. 2, pp. 174–188, Feb. 2002.

[38] M. Lentmaier, B. Krach, and P. Robertson, "Bayesian time delay estimation of GNSS signals in dynamic multipath environments," International Journal of Navigation and Observation, vol. 2008, Mar. 2008, doi:10.1155/2008/372651.